Unconventional magnetism in the layered oxide LaSrRhO$_4$

Noriyasu Furuta, Shinichiro Asai, Taichi Igarashi, Ryuji Okazaki, Yukio Yasui,[*] and Ichiro Terasaki[†]

Department of Physics, Nagoya University, Nagoya 464-8602, Japan

Masami Ikeda, Takahito Fujita, and Masayuki Hagiwara

KYOKUGEN (Center for Quantum Science and Technology under Extreme Conditions), Osaka University, Toyonaka, Osaka 560-8531, Japan

Kensuke Kobayashi, Reiji Kumai, Hironori Nakao, and Youichi Murakami

Condensed Matter Research Center and Photon Factory, Institute of Materials Structure Science, High Energy Accelerator Research Organization, Tsukuba 305-0801, Japan

We have prepared polycrystalline samples of LaSrRh$_{1-x}$Ga$_x$O$_4$ and LaSr$_{1-x}$Ca$_x$RhO$_4$, and have measured the x-ray diffraction, resistivity, Seebeck coefficient, magnetization, and electron spin resonance in order to evaluate their electronic states. The energy gap evaluated from the resistivity and the Seebeck coefficient systematically changes with the Ga concentration, and suggests that the system changes from a small polaron insulator to a band insulator. We find that all the samples show Curie-Weiss-like susceptibility with a small Weiss temperature of the order of 1 K, which is seriously incompatible with the collective wisdom that a trivalent rhodium ion is nonmagnetic. We have determined the g factor to be $g = 2.3$ from the electron spin resonance, and the spin number to be $S = 1$ from the magnetization-field curves by fitting with a modified Brillouin function. The fraction of the $S = 1$ spins is 2%–5%, which depends on the degree of disorder in the La/Sr/Ca site, which implies that disorder near the apical oxygen is related to the magnetism of this system. A possible origin for the magnetic Rh^{3+} ions is discussed.

PACS number(s): 75.20.Hr, 75.30.Wx, 72.20.−i

I. INTRODUCTION

The 3d transition-metal oxides have been extensively studied as a gold mine for functional materials, which is exemplified by the ferroelectricity in titanium oxides, the magnetoresistivity and multiferroelectricity in manganese oxides, the thermoelectricity in cobalt oxides, and the high-temperature superconductivity in copper oxides. In contrast, the 4d transition metal oxides have been less investigated as functional materials. While magnetism is a fertile source for the functions in the 3d transition-metal oxides, the 4d transition-metal oxides are often paramagnetic except for some insulating ruthenium oxides [1–3] This comes from different spin states between 3d and 4d elements.

The spin state is a fundamental concept in transition-metal compounds/complexes [4]. In a transition-metal ion surrounded with octahedrally coordinated oxygen anions, the fivefold degenerate d orbitals in vacuum are split into the triply degenerate t_{2g} (xy, yz, and zx) orbitals and the doubly degenerate e_g ($x^2 - y^2$ and z^2) orbitals, and the energy gap between the t_{2g} and e_g levels called the ligand-field gap often competes with the Hund coupling. When the ligand field gap is larger, the d electrons first occupy the t_{2g} states to minimize the total spin number. On the other hand, when the Hund coupling is strong, the total spin number is maximized. The former state is called the low spin state, and the latter the high spin state.

Rhodium is located below cobalt in the Periodic Table, and thus is expected to have similar chemical properties. In fact,

many cobalt oxides have their isomorphic rhodium oxides, and similar transport properties are reported [5–10]. We have studied the Rh substitution effects on LaCoO$_3$, and found that LaCo$_{0.8}$Rh$_{0.2}$O$_3$ exhibits a ferromagnetic transition below 18 K [11]. The substituted Rh ions tend to stabilize high-spin state Co^{3+} ions in the samples [12,13], and such high-spin state Co^{3+} ions interact with each other at low temperatures to cause the ferromagnetic order. This clearly indicates that the Rh^{3+} ion is *not* a simple nonmagnetic element.

In this paper, we focus on the layered rhodium oxide LaSrRhO$_4$. This oxide crystallizes in the K$_2$NiF$_4$-type (A_2BO_4-type) structure, where 50% La and 50% Sr make a solid solution in the A site. The corner-shared RhO$_6$ octahedra form the RhO$_2$ plane along the ab plane, and alternately stack with the (La/Sr)$_2$O$_2$ layer. Shimura *et al.* [14] measured the physical properties of Sr$_{2-x}$La$_x$RhO$_4$, and found a small amount of paramagnetic contribution, although the formal valence of Rh was 3+. This is highly unusual, because Rh^{3+} is believed to be highly stable in the low-spin state ($S = 0$). Here we present measurements and analyses of the transport and magnetic properties of LaSrRh$_{1-x}$Ga$_x$O$_4$ and LaSr$_{1-x}$Ca$_x$RhO$_4$, and show that 2%–5% of the Rh^{3+} ions act as $S = 1$. We discuss a possible mechanism to create the magnetic Rh^{3+} ions based on the experimental results.

II. EXPERIMENT

Polycrystalline samples of LaSrRh$_{1-x}$Ga$_x$O$_4$ ($x = 0$, 0.1, 0.2, 0.3, 0.4, 0.5, 0.6, 0.7, 0.8, and 0.9) and LaSr$_{1-x}$Ca$_x$RhO$_4$ ($x = 0.1$, 0.2, and 0.3) were prepared by a conventional solid state reaction method. High-purity (99.9%) oxide powders of Rh$_2$O$_3$, Ga$_2$O$_3$, La$_2$O$_3$, SrCO$_3$, and CaCO$_3$ were used as raw materials. Stoichiometric mixtures of these powders were

ground, and were calcined for 24 h at 1200 °C in air. The calcined powder was then ground, pressed into pellet, and sintered 48 h at 1300 °C in air.

X-ray diffraction was measured with a Rigaku Geigerflex (Cu $K\alpha$ radiation). Synchrotron x-ray diffraction was taken for a powder sample of $x = 0.5$ with a wavelength of 0.6887 Å at BL-8A, KEK-PF, Japan. Rietveld refinement was conducted using Rietan 2000 code [15]. Resistivity was measured in a four probe configuration in a constant voltage applied across a series circuit of a sample and a standard resistance. The Seebeck coefficient was measured in a two-probe configuration in a steady state technique with a typical temperature gradient of 1 K/cm. A contribution of the voltage leads was carefully subtracted. Magnetization was measured using a superconducting quantum interference device magnetometer (Quantum Design MPMS) from 5 to 300 K. External magnetic field $\mu_0 H$ was chosen to be from 1 to 5 T, depending on the magnetization of the samples. The field dependence of the magnetization was measured for LaSrRhO$_4$ at 2, 5, and 10 K in sweeping $\mu_0 H$ from 0 to 7 T. Electron spin resonance (ESR) was measured in static magnetic fields from 0 to 14 T in the frequency range from 90 to 200 GHz, and nonresonant transmission signal was detected using a vector network analyzer in sweeping magnetic fields. For frequencies of 27.5 and 34 GHz, a cavity perturbation technique was employed.

III. RESULTS AND DISCUSSION

Figure 1(a) shows typical x-ray diffraction patterns for the prepared samples. We find that LaSrRhO$_4$ ($x = 0$) and LaSrGaO$_4$ ($x = 1$) make a solid solution in the whole range of x. All the peaks for $x = 0$ are indexed as the orthorhombic structure with the space group $Fmmm$, as is consistent with preceding papers [14,16]. With increasing Ga content x, the symmetry changes from orthorhombic to tetragonal around $x = 0.3$, as is evidenced by the small peaks around $2\theta = 23°$ and $28°$ for $x = 0.6$. This tetragonal structure is consistent with the other end phase of LaSrGaO$_4$ with the space group of $I4/mmm$ [17]. Possibly owing to the symmetry change, the c axis length shown in Fig. 1(c) takes a minimum around $x = 0.3$, while the a and b axis lengths shown in Fig. 1(b) rather smoothly decrease with x. Since a Ga^{3+} ion has a smaller ionic radius than a Rh^{3+} ion, the lattice volume smoothly decreases with x (not shown).

The title compound belongs to the Ruddlesden-Popper series of (La,Sr)$_{n+1}$(Rh,Ga)$_n$O$_{3n+1}$, and $n \neq 1$ phases often grow as a secondary phase. In the present case, (La,Sr)(Rh,Ga)O$_3$ ($n = \infty$) can grow in the same preparation conditions, and a small amount of such impurity may change the valence of the rhodium ion from 3+. In order to check this possibility, we have measured synchrotron x-ray diffraction for the $x = 0.5$ sample. Figure 2 shows the synchrotron x-ray diffraction pattern at room temperature. There are some unindexed reflections around 12°, but their intensity is less than 0.6% of the main peak. We performed the Rietveld refinement, and find that the resultant fitting is reasonably well. Thus we safely conclude that the prepared powder samples are stoichiometric and in single phase within an uncertainty of less than 0.6%.
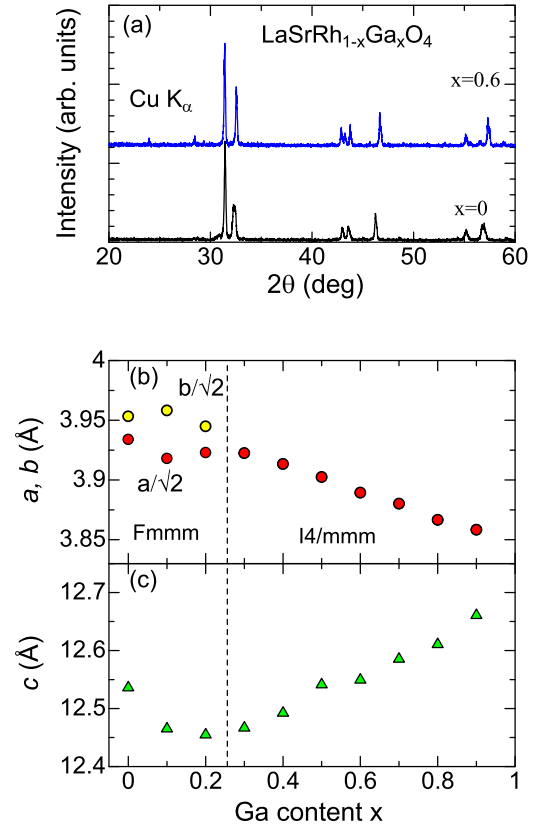

FIG. 1. (Color online) (a) X-ray diffraction patterns of LaSrRh$_{1-x}$Ga$_x$O$_4$ ($x = 0$ and 0.6). (b), (c) Lattice parameters plotted as a function of the Ga content x. The space group changes from orthorhombic ($Fmmm$) to tetragonal ($I4/mmm$) between $x = 0.2$ and 0.3.

Next we evaluate the valence of the rhodium ion from the transport properties. Figure 3(a) shows the resistivity of LaSrRh$_{1-x}$Ga$_x$O$_4$ plotted as a function of inverse temperature. The room-temperature resistivity is 1 Ω cm for $x = 0$, which is
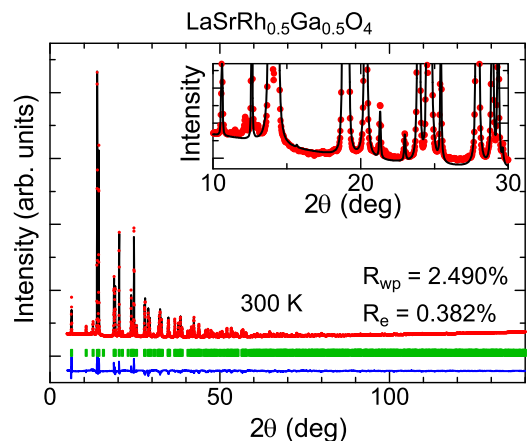

FIG. 2. (Color online) Rietveld refinement for the x-ray diffraction patterns of LaSrRh$_{0.5}$Ga$_{0.5}$O$_4$. The inset shows an extended figure from $2\theta = 10°$ to 30°. Although a tiny amount of unindexed peak is seen around 12°, the refinement excellently reproduces the observed data.
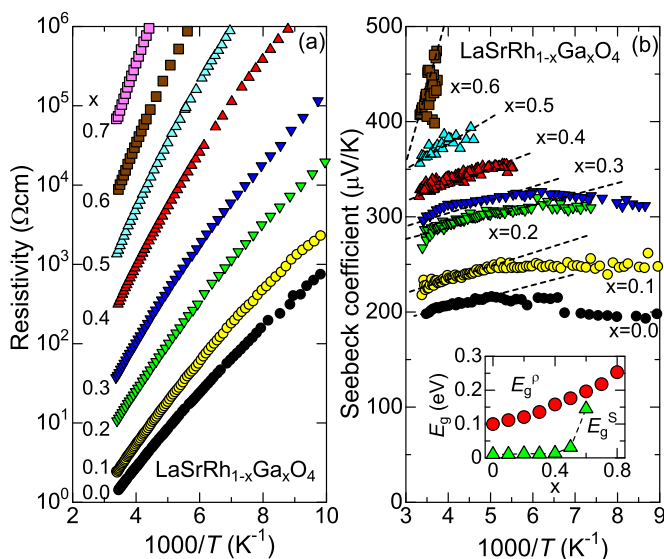
FIG. 3. (Color online) (a) Resistivity and (b) the Seebeck coefficients of the prepared samples. The dotted lines in (b) are guides to the eye. The inset in (b) shows the energy gap evaluated from the resistivity (E_g^ρ) and the Seebeck coefficient (E_g^S).

FIG. 4. (Color online) Magnetic susceptibility of LaSrRh$_{1-x}$Ga$_x$O$_4$. All the data exhibits Curie-Weiss–like paramagnetism. The data for the cubic Rh oxide LaRh$_{0.5}$Ga$_{0.5}$O$_3$ is also plotted. The paramagnetic signal is far smaller, indicating that the paramagnetism is inherent in the layered structure.

higher than the previously reported data by Shimura *et al.* [14]. Figure 3(b) shows the Seebeck coefficient of LaSrRh$_{1-x}$Ga$_x$O$_4$ plotted as a function of inverse temperature. Again, the room-temperature thermopower for $x = 0$ is larger than the data by Shimura *et al.* [14]. These results indicate that the carrier concentration of our sample is lower than that of their samples. The positive sign of the Seebeck coefficient indicates that the valence of the rhodium ion is larger than 3. Considering the fraction of the impurity phase is less than 0.6%, the valence of the rhodium ions ranges from 3.00 to 3.02. Note that the Heikes formula [18] is not valid in the present case because of significant temperature variation. The isostructural LaSrCoO$_4$ shows nearly the same value of 200 μV/K at 300 K with strong temperature variation [19].

Let us have a closer look at the compositional dependence of the transport data. The resistivity increases with increasing Ga content, and the slope in the Arrhenius plot increases concomitantly. The energy gap (E_g^ρ) determined by the slope is plotted in the inset of Fig. 3(b); the magnitude is 0.1–0.3 eV, which is typical for insulating transition-metal oxides. Since the $x = 1$ sample has a band gap larger than 3 eV, the increase in E_g^ρ indicates a systematic evolution of the electronic states. The Seebeck coefficient increases with decreasing temperature around room temperature, suggesting an activation-type transport. By evaluating the slope of the Seebeck coefficient against $1/T$ shown by the dotted lines, we determine the energy gap (E_g^S) as is also plotted in the inset of Fig. 3(b). $E_g^\rho \gg E_g^S$ for $x < 0.5$ indicates that the activation energy predominantly comes from the mobility, and the system is well described in terms of small polaron [20]. On the contrary, $E_g^\rho \sim E_g^S$ for $x = 0.6$ indicates that the activation energy comes from the energy gap in the density of states. This indicates that the system continuously evolves from a small polaron insulator to a band insulator. We further note that the
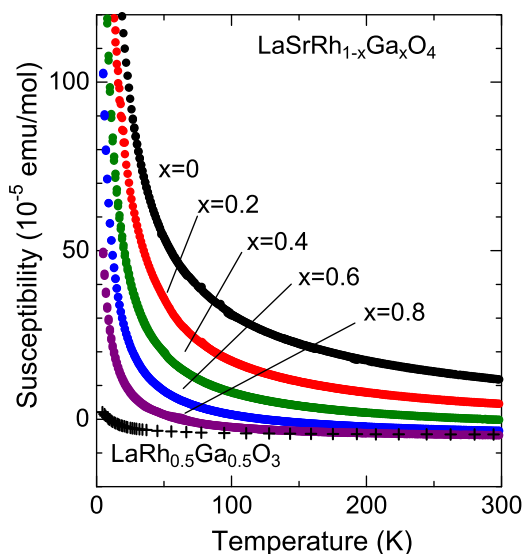
unwanted holes are negligible for $x > 0.5$ at low temperatures because of the gap in the density of states.

Now we focus on the magnetism of our samples. Figure 4 shows the susceptibility of LaSrRh$_{1-x}$Ga$_x$O$_4$. A first thing to note is that *all the samples are paramagnetic*. Considering that Sr^{2+}, La^{3+}, and Ga^{3+} ions are diamagnetic, we have come to the conclusion that Rh^{3+} is *magnetic*, which is seriously incompatible with our collective wisdom. A second feature is that all the data are roughly inversely proportional to temperature, suggesting that the magnetic moment on the Rh^{3+} ion is independent from each other. A third feature is that the temperature-independent susceptibility is significant, and changes its sign with x. We also emphasize that the susceptibility of the cubic Rh^{3+} oxide LaRh$_{0.5}$Ga$_{0.5}$O$_3$ shows a much smaller paramagnetic signal. This indicates that the paramagnetic response of LaSrRh$_{1-x}$Ga$_x$O$_4$ is inherent in the layered structure of A_2BO_4, and does not come from impurities in the raw powdered oxides of Rh$_2$O$_3$, La$_2$O$_3$, and Ga$_2$O$_3$.

Considering the above features, we fit the experimental data with a modified Curie-Weiss law given by

$$\chi = \frac{C}{T + \theta} + \chi_0, \qquad (1)$$

where C, θ, and χ_0 are the Curie constant, the Weiss temperature, and the temperature-independent susceptibility, respectively. As shown in Fig. 5(a), the inverse susceptibility $(\chi - \chi_0)^{-1}$ is found to be linear in T down to the lowest temperature measured. Figures 5(b)–5(d) show the fitting parameters. As expected, the Weiss temperature is determined to be a small value of the order of 1 K. Thus, except for low temperatures, the spin-spin interaction can be neglected. The Curie constant is 0.02 emu K/mol for $x = 0$, which is 3% of that observed in LaSrCoO$_4$ [19,21–23]. This implies that only 3% of the Rh ions are magnetic. It should be emphasized that all the Curie constants decrease almost linearly with x
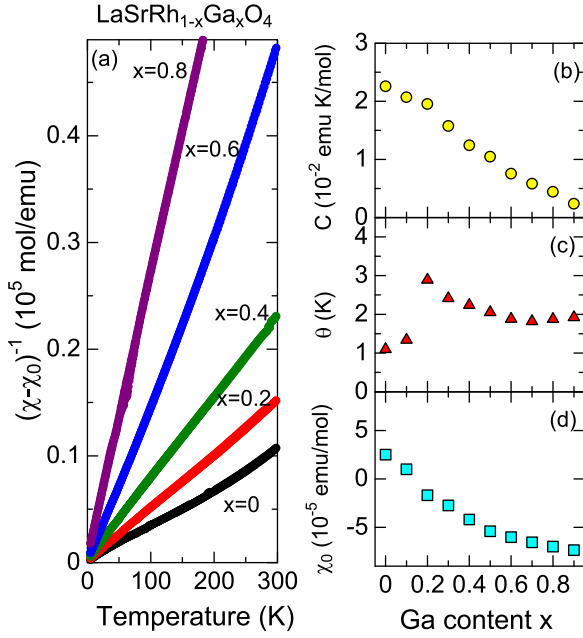
FIG. 5. (Color online) (a) Inverse susceptibility of LaSrRh$_{1-x}$Ga$_x$O$_4$ plotted as a function of temperature. Note that the temperature-independent susceptibility χ_0 is subtracted. (b)–(d) The parameters obtained from the susceptibility in Fig. 4 by fitting with the Curie-Weiss law. (b) The Curie constant, (c) the Weiss temperature, and (d) the temperature independent susceptibility χ_0.
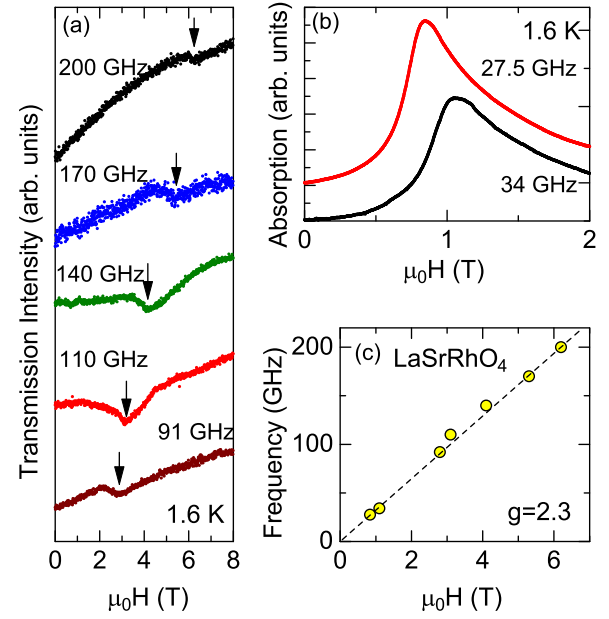

FIG. 6. (Color online) (a) Millimeter-wave adsorption by electron spin resonance measured with a nonresonant transmission at 1.6 K in LaSrRhO$_4$. The arrows indicate the resonance field. (b) Microwave absorption using cavity perturbation with resonance frequencies of 27.5 and 34 GHz. (c) Resonance frequency plotted as a function of external field. From the slope, the g value is evaluated to be 2.3.

[Fig. 5(b)], which implies that the Ga substitution simply causes a dilution effect, and the magnetic Rh ions are always 3% of the Rh ions for all the samples. We should emphasize that the fraction of 3% is much larger than the purity of the raw-material powders and the volume fraction of impurity phases evaluated above. In addition, we can neglect thermally activated Rh^{4+} ions for $x > 0.5$ at low temperature because of the finite energy gap in the density of states (the inset of Fig. 3), and yet observe the Curie-Weiss behavior.

Figure 6(a) shows the millimeter-wave transmission intensity of LaSrRhO$_4$ plotted as a function of external field $\mu_0 H$ at 1.6 K. As indicated by the arrows, all the transmission curves have a broad dip, which corresponds to electron spin resonance at the field. The field at which the dip is observed increases with increasing frequency. The dip width is as large as 1 T, suggesting a short spin-lattice relaxation time in this system. Figure 6(b) shows the absorption curve measured with resonant cavities for 27.5 and 34 GHz at 1.6 K. An absorption peak is clearly visible near 1 T with a broad width of 1 T. We should note that the shape of the absorption curve is not symmetric to the resonance field. Such an asymmetric shape has been analyzed with a Dysonian function [24], but the fitting was not satisfactory for the present data (not shown). At present, we do not understand the origin for the absorption asymmetry, but we speculate that the resonance condition seems to change with increasing external fields, which implies that the dielectric constant may depend on magnetic field.

Figure 6(c) shows the resonance frequency plotted as a function of resonance field. As is clearly seen, the frequency ν is linear in magnetic field $\mu_0 H$ within experimental errors. This is indeed what is expected in electron spin resonance

for a noninteracting spin system, and is consistent with the very small θ in Fig. 5(c). We obtain the g value from the proportionality constant expressed by $h\nu = g\mu_B\mu_0 H$ to be $g = 2.3$. This value indicates that orbital angular moment L is quenching. The perovskite oxide LaCoO$_3$ shows a g value of 3.35 [25], which is explained in terms of $L = 1$ in t_{2g} orbitals. Thus the value of $g = 2.3$ excludes the possibility that the Rh^{3+} is in the high-spin state.

Next let us examine the spin state of the Rh ions responsible from the field dependence of the magnetization. Since the electron configuration of Rh^{3+} is $(4d)^6$, a possible magnetic state is the intermediate-spin state ($S = 1$) or the high-spin state ($S = 2$). Thanks to the weak spin-spin interaction, we can employ the Brillouin function for the fitting, with which we can distinguish $S = 1$ from $S = 2$. Figure 7 shows the magnetization-field curves of LaSrRhO$_4$ taken at 2, 5, and 10 K. The magnetization shows saturation behavior in high fields, which is more significant at lower temperature. This is qualitatively the same as is expected from the Brillouin function. Considering the small value of θ, we slightly modify the Brillouin function to include the magnetization M from the spin-spin interaction, and propose a following function given by

$$B_S^*(H,M) = \frac{\sum -g\mu_B S_z \exp[-\beta g\mu_B S_z \mu_0(H-\alpha M)]}{\sum \exp[-\beta g\mu_B S_z \mu_0(H-\alpha M)]}, \quad (2)$$

where α is the molecular field coefficient given by $\alpha = \theta/C$, and β is the inverse temperature $\beta = 1/k_B T$. Thus the magnetization M is determined by the following self consistent
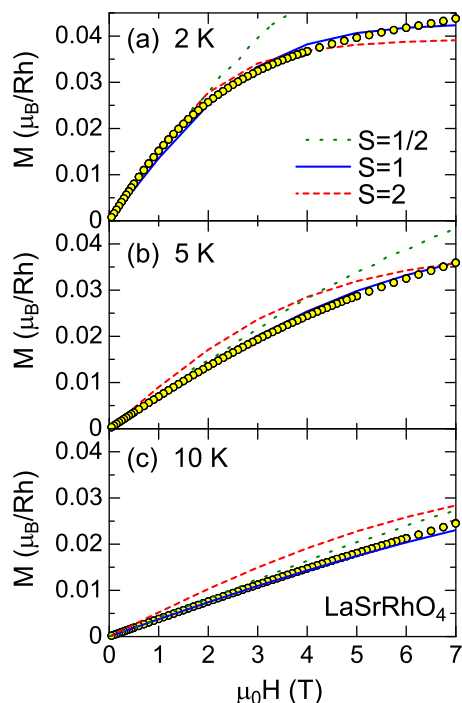
FIG. 7. (Color online) Magnetization-field curves of LaSrRhO$_4$ fitted with a modified Brillouin function (see text). (a) 2 K, (b) 5 K, and (c) 10 K. The open circles represent the measured magnetization, and the solid, broken, and dotted curves are numerically calculated curves for $S = 1$, $S = 2$, and $S = 1/2$, respectively. The calculated curves are drawn to fit the low-field magnetization at 2 K.

equation expressed as

$$M = f N_0 B_S^*(H, M) + \chi_0 H, \qquad (3)$$

where f is the fraction of the magnetic Rh^{3+} ions. We take α and χ_0 from the data in Fig. 5, and $g = 2.3$ from Fig. 6. Consequently, the fraction f is left as the only one adjustable parameter. The solid, broken, and dotted curves in Fig. 7 represent the calculations for $S = 1$, $S = 2$, and $S = 1/2$, respectively. The adjustable parameter f is taken to be 1.9% for $S = 1$, 0.85% for $S = 2$, and 4.7% for $S = 1/2$, in order to fit low-field magnetization at 2 K. As is clearly seen in Fig. 7, the $S = 1$ curves consistently explain the measured magnetization. The large deviation of the calculated $S = 1/2$ curve clearly excludes a possibility that some Rh^{3+} ions may be disproportionated as Rh^{2+} and Rh^{4+} to work as $S = 1/2$.

In order to examine the A-site disorder effect, we prepared a set of samples of LaSr$_{1-x}$Ca$_x$RhO$_4$. Figure 8 shows the inverse susceptibility $(\chi - \chi_0)^{-1}$ of LaSr$_{1-x}$Ca$_x$RhO$_4$ plotted as a function of temperature. The temperature-independent susceptibility χ_0 is 1.8, 1.5, 1.3, and 0.8 × 10^{-5} emu/mol for $x = 0$, 0.1, 0.2, and 0.3, respectively. Unlike the susceptibility of LaSrRh$_{1-x}$Ga$_x$O$_4$, the slope of the susceptibility increases with the Ca content x. By fitting the susceptibility with Eq. (1), we obtain the Curie constant C, from which we evaluate the fraction of the magnetic Rh^{3+} through the relation as

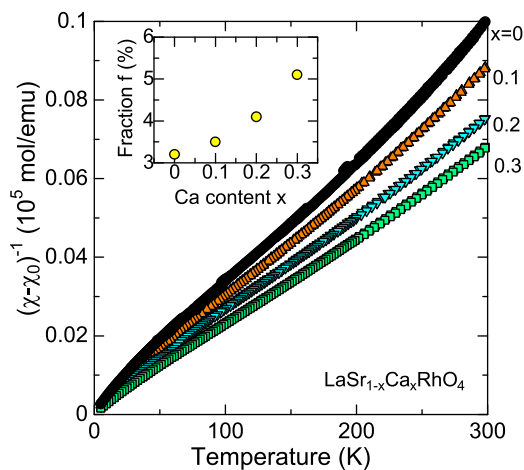$$C = \frac{f N_0 g^2 S(S+1) \mu_B^2}{3 k_B}. \qquad (4)$$

FIG. 8. (Color online) Inverse susceptibility $(\chi - \chi_0)^{-1}$ of LaSr$_{1-x}$Ca$_x$RhO$_4$ plotted as a function of temperature. The temperature-independent susceptibility χ_0 is 1.8, 1.5, 1.3, and 0.8 × 10^{-5} emu/mol for $x = 0$, 0.1, 0.2, and 0.3, respectively. The slope changes significantly with the Ca content x. The intermediate spin state for the tetragonally distorted octahedra is schematically shown in the inset. Fraction of the magnetic Rh^{3+} ions evaluated from the slope is shown in the inset.

By putting $g = 2.3$ and $S = 1$, we get the fraction f as shown in the inset of Fig. 8. We notice that for $x = 0$, the fraction of 3.1% evaluated from Eq. (4) is slightly larger than 1.9% evaluated from Eq. (3). Normally, the g value is determined by ESR accurately, but the distorted signal makes it impossible this time. Since the g value is determined to be 2.3 ± 0.1, the disagreement in the fraction may come from the ambiguity in the C value. An important feature is that the fraction increases with the Ca content x, which implies that the magnetic Rh^{3+} ions are related to the degree of the A-site disorder.

Finally, let us discuss a possible origin of the magnetic Rh^{3+} ions distributed with a fraction of 2%–5%. A first point is that their magnetic moment is stable at all temperature measured, and the number of the magnetic ions is independent of temperature, for the susceptibility obeys the Curie-Weiss law with a small Weiss temperature in a wide range of temperature. A second point is that the magnetic Rh^{3+} is local, just like a magnetic impurity, and the fraction is almost independent of the B-site disorder, but depends on the A-site disorder. A third point is that such magnetic signal is related to the layered structure, possibly related to the tetragonal distortion of the RhO$_6$ octahedron. Note that the susceptibility of LaRh$_{0.5}$Ga$_{0.5}$O$_3$ has a negligibly small Curie tail as shown in Fig. 4.

Attfield et al. have discovered that the A-site disorder seriously affects the superconducting transition temperature in the doped La$_2$CuO$_4$ [26]. Since the transition temperature is sensitive to the bond length of Cu^{2+} and apical O^{2-} ions [27], the variance in the out-of-plane Cu-O distance may deteriorate the superconducting properties. We apply a similar story to the title compound. When the Rh-O bond length ξ along the c axis direction is sufficiently short, we can regard RhO$_6$ as a regular octahedron, where the low spin state is stable [the left schematic in Fig. 9(a)]. On the other hand,
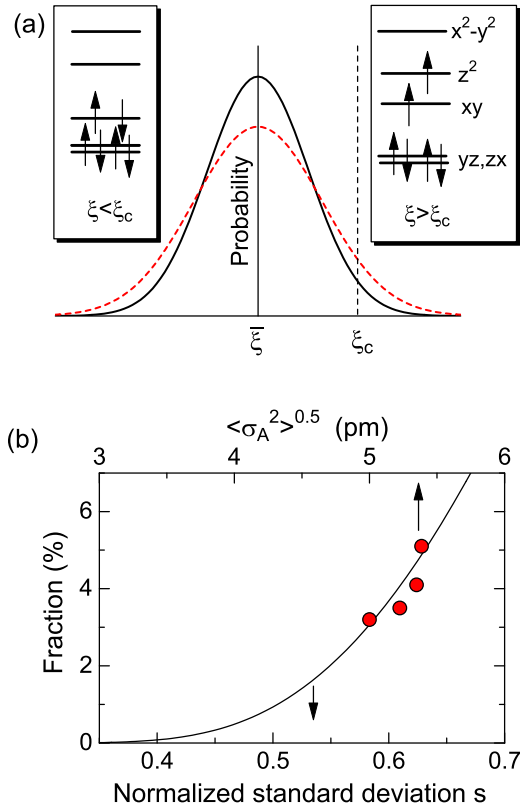
FIG. 9. (Color online) (a) Possible distribution of the bond length ξ of the Rh ion and the apical oxygen ion. When ξ exceeds a critical value of ξ_c, the energy gap of xy and z^2 becomes small enough to stabilize the intermediate spin state. For $\xi < \xi_c$, the low spin state is favored. The fraction of the intermediate spin is larger in a more disordered distribution (the dotted curve). (b) The theoretical curve for the fraction plotted as a function of the normalized standard deviation s given by Eq. (11). The observed fraction is also plotted as a function of the A-site disorder $\langle \sigma_A^2 \rangle \equiv \langle r_A^2 \rangle - \langle r_A \rangle^2$, where r_A is the ionic radius of the A site ions (see text).

when ξ exceeds a critical value of ξ_c, a long ξ largely splits the energy level between $x^2 - y^2$ and z^2, and eventually shifts the z^2 level downwards. Likewise, it also largely splits the energy level between xy and yz/zx, and raises the xy level. As a result, a small energy gap between the z^2 and xy levels will favor the spin state shown in the right schematic in Fig. 9(a). This configuration is identical to the intermediate spin state proposed for LaSrCoO$_4$ [28].

We will roughly estimate how the fraction f of the magnetic moment is related to the disorderness of the A-site cation. Assuming a Gaussian distribution with the mean value $\bar{\xi}$ and the variance σ^2, $f \equiv f(\bar{\xi}, \sigma^2)$ equals the probability for $\xi > \xi_c$

given by

$$f(\bar{\xi}, \sigma^2) = \frac{1}{\sqrt{2\pi\sigma^2}} \int_{\xi_c}^{\infty} \exp\left(-\frac{(x - \bar{\xi})^2}{2\sigma^2}\right) dx. \quad (5)$$

By replacing the variable $t = (x - \bar{\xi})/\sqrt{2\sigma^2}$, we get

$$f(\bar{\xi}, \sigma^2) = \frac{1}{\sqrt{\pi}} \int_{\Delta\xi/\sqrt{2\sigma^2}}^{\infty} \exp(-t^2) dt \quad (6)$$

$$= 2 \operatorname{erfc}\left(\frac{\Delta\xi}{\sqrt{2\sigma^2}}\right), \quad (7)$$

where erfc(t) is the complementary error function and $\Delta\xi = \xi_c - \bar{\xi}$. If we assume $\bar{\xi}$ to be independent of the Ca concentration in LaSr$_{1-x}$Ca$_x$CoO$_4$, we find $s \equiv \sqrt{2\sigma^2}/\Delta\xi$ is the only parameter, and the fraction is described simply as

$$f(s) = 2 \operatorname{erfc}\left(\frac{1}{s}\right). \quad (8)$$

Figure 9(b) depicts such a relationship, where the fraction $f(s)$ is plotted from $s = 0.35$ to 0.7. One can see that $f(s)$ is a monotonically increasing function of s, and the fraction increases with the variance in the Rh-O bond. We also plot the standard deviation in the A-site ionic radius as $\sqrt{\sigma_A^2} = \sqrt{\langle r_A^2 \rangle - \langle r_A \rangle^2}$ in the same graph. Although this quantity does not equal the standard deviation in the Rh-O distance, one can see that $\sqrt{\sigma_A^2}$ roughly follows the curve given by Eq. (8).

IV. SUMMARY

We have prepared a set of polycrystalline samples of LaSrRh$_{1-x}$Ga$_x$O$_4$ and LaSr$_{1-x}$Ca$_x$RhO$_4$, and have measured the resistivity, Seebeck coefficient, magnetization, and electron spin resonance in order to evaluate the magnetic properties and spin states of the layered rhodium oxides. We find that all the samples show Curie-Weiss–like susceptibility with a small Weiss temperature of the order of 1 K, which is seriously incompatible with the collective wisdom that a trivalent rhodium ion is nonmagnetic. The g factor is determined to be $g = 2.3$ from the electron spin resonance, and the spin number is determined as $S = 1$ from the magnetization-field curves by fitting with a modified Brillouin function. The fraction of the $S = 1$ spins is 2%–5%, and the disorder in the La/Sr/Ca site determines the spin fraction.

[1] M. Subramanian, G. Aravamudan, and G. S. Rao, Prog. Solid State Chem. **15**, 55 (1983).

[2] P. Battle and W. Macklin, J. Solid State Chem. **52**, 138 (1984).

[3] S. Nakatsuji, S. Ikeda, and Y. Maeno, J. Phys. Soc. Jpn. **66**, 1868 (1997).

[4] S. Sugano, Y. Tanabe, and H. Kamimura, *Multiplets of Transition-metal Ions in Crystals* (Academic Press, New York, 1970).

[5] S. Okada and I. Terasaki, Jpn. J. Appl. Phys. **44**, 1834 (2005).

[6] S. Okada, I. Terasaki, H. Okabe, and M. Matoba, J. Phys. Soc. Jpn. **74**, 1525 (2005).

[7] Y. Klein, S. Hébert, D. Pelloquin, V. Hardy, and A. Maignan, Phys. Rev. B **73**, 165121 (2006).

[8] Y. Okamoto, M. Nohara, F. Sakai, and H. Takagi, J. Phys. Soc. Jpn. **75**, 023704 (2006).

[9] S. Shibasaki, W. Kobayashi, and I. Terasaki, Phys. Rev. B **74**, 235110 (2006).

[10] A. Maignan, V. Eyert, C. Martin, S. Kremer, R. Frésard, and D. Pelloquin, Phys. Rev. B **80**, 115103 (2009).

[11] S. Asai, N. Furuta, Y. Yasui, and I. Terasaki, J. Phys. Soc. Jpn. **80**, 104705 (2011).

[12] K. Knizek, J. Hejtmánek, M. Marysko, Z. Jirák, and J. Bursik, Phys. Rev. B **85**, 134401 (2012).

[13] S. Asai, N. Furuta, R. Okazaki, Y. Yasui, and I. Terasaki, Phys. Rev. B **86**, 014421 (2012).

[14] T. Shimura, M. Itoh, Y. Inaguma, and T. Nakamura, Phys. Rev. B **49**, 5591 (1994).

[15] F. Izum and K. Momma, Solid State Phenom. **130**, 15 (2007).

[16] G. Blasse, J. Inorg. Nucl. Chem. **27**, 2683 (1965).

[17] J. F. Britten, H. A. Dabkowska, A. B. Dabkowski, J. E. Greedan, J. L. Campbell, and W. J. Teesdale, Acta Crystallogr. C **51**, 1975 (1995).

[18] P. M. Chaikin and G. Beni, Phys. Rev. B **13**, 647 (1976).

[19] A. V. Chichev, M. Dlouhá, S. Vratislav, K. Knížek, J. Hejtmánek, M. Maryško, M. Veverka, Z. Jirák, N. O. Golosova, D. P. Kozlenko, and B. N. Savenko, Phys. Rev. B **74**, 134414 (2006).

[20] T. T. M. Palstra, A. P. Ramirez, S. W. Cheong, B. R. Zegarski, P. Schiffer, and J. Zaanen, Phys. Rev. B **56**, 5104 (1997).

[21] Y. Moritomo, K. Higashi, K. Matsuda, and A. Nakamura, Phys. Rev. B **55**, R14725 (1997).

[22] Y. Shimada, S. Miyasaka, R. Kumai, and Y. Tokura, Phys. Rev. B **73**, 134424 (2006).

[23] R. Ang, Y. P. Sun, X. Luo, C. Y. Hao, and W. H. Song, J. Phys. D: Appl. Phys. **41**, 045404 (2008).

[24] J. P. Joshi and S. V. Bhat, J. Magn. Reson. **168**, 284 (2004).

[25] S. Noguchi, S. Kawamata, K. Okuda, H. Nojiri, and M. Motokawa, Phys. Rev. B **66**, 094404 (2002).

[26] J. P. Attfield, A. L. Kharlanov, and J. A. McAllister, Nature (London) **394**, 157 (1998).

[27] Y. Ohta, T. Tohyama, and S. Maekawa, Phys. Rev. B **43**, 2968 (1991).

[28] X. L. Wang and E. Takayama-Muromachi, Phys. Rev. B **72**, 064401 (2005).